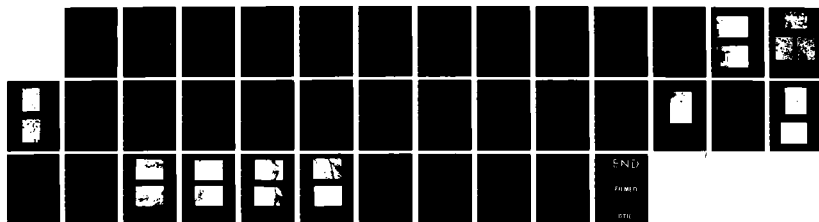ORDERED CARBON - METAL ALLOYS FOR EXTRATERRESTRIAL
POWER SYSTEMS(U) AUBURN UNIV AL DEPT OF MECHANICAL
ENGINEERING B A CHIN ET AL. 09 AUG 85 AFOSR-TR-85-1041

END

FILMED
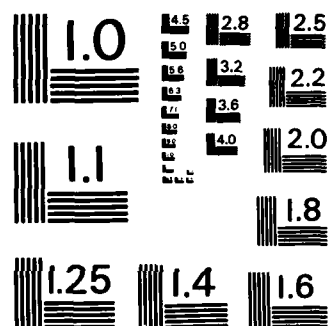
DTIC

MICROCOPY RESOLUTION TEST CHART

NATIONAL BUREAU OF STANDARDS-1963-A

AFOSR-TR- 85-1041

ORDERED CARBON - METAL ALLOYS FOR

EXTRATERRESTRIAL POWER SYSTEMS

Interim Progress Report - Second Year

AFOSR Grant: 83-0168

B. A. Chin
N. H. Madsen
K. C. Yeh
P. F. Gills

Department of Mechanical Engineering
Auburn University, AL 36849
Phone: (205) 826-4820

REPORT DOCUMENTATION PAGE

A162287

1a. REPORT SECURITY CLASSIFICATION		1b. RESTRICTIVE MARKINGS		
Unclassified		None		
2a. SECURITY CLASSIFICATION AUTHORITY		3. DISTRIBUTION/AVAILABILITY OF REPORT		
2b. DECLASSIFICATION/DOWNGRADING SCHEDULE		Not Restricted Approved for public release; distribution unlimited.		
N/A				
4. PERFORMING ORGANIZATION REPORT NUMBER(S)		5. MONITORING ORGANIZATION REPORT NUMBER(S)		
AFOSR-83-0168-2		AFOSR-TR- 1041		
6a. NAME OF PERFORMING ORGANIZATION	6b. OFFICE SYMBOL (If applicable)	7a. NAME OF MONITORING ORGANIZATION		
Auburn University	N/A	AFOSR/NE		
6c. ADDRESS (City, State and ZIP Code)		7b. ADDRESS (City, State and ZIP Code)		
Department of Mechanical Engineering Auburn, AL 36849		Building 410 Bolling AFB, D.C. 20332-6448		
8a. NAME OF FUNDING/SPONSORING ORGANIZATION	8b. OFFICE SYMBOL (If applicable)	9. PROCUREMENT INSTRUMENT IDENTIFICATION NUMBER		
AFOSR/NE	NE	Grant # AFOSR-83-0168		
8c. ADDRESS (City, State and ZIP Code)		10. SOURCE OF FUNDING NOS.		

8c. ADDRESS (City, State and ZIP Code)	PROGRAM ELEMENT NO.	PROJECT NO.	TASK NO.	WORK UNIT NO.
Building 410 Bolling AFB, D.C. 20332-6448	61102F	2306	A2	

11. TITLE (Include Security Classification)				
Ordered Carbon Metal Alloys for Extraterrestrial Power Systems				

12. PERSONAL AUTHOR(S)
Bryan A. Chin, N. H. Madsen, K. C. Yeh, P. F. Gills

13a. TYPE OF REPORT	13b. TIME COVERED		14. DATE OF REPORT (Yr., Mo., Day)	15. PAGE COUNT
Annual	FROM 6/84 TO 6/85		85/8/9	33

16. SUPPLEMENTARY NOTATION
N/A

17.	COSATI CODES		18. SUBJECT TERMS (Continue on reverse if necessary and identify by block number)
FIELD	GROUP	SUB. GR.	
Material	Alloys	Mech. Proper.	High Temperature, Alloys, Mechanical Properties

19. ABSTRACT (Continue on reverse if necessary and identify by block number)

The objective of this research is to investigate a new class of material composed of 30-60 atomic percent (C-Ti) for ultrahigh temperature applications in space power systems. The alloy system under investigation exhibits melting temperatures in excess of 2500 degrees C and form long range ordered structures which are expected to yield materials with exceptional high temperature strength and resistance to environmental degradation.

20. DISTRIBUTION/AVAILABILITY OF ABSTRACT	21. ABSTRACT SECURITY CLASSIFICATION	
UNCLASSIFIED/UNLIMITED ☒ SAME AS RPT. ☐ DTIC USERS ☐	Unclassified	
22a. NAME OF RESPONSIBLE INDIVIDUAL	22b. TELEPHONE NUMBER (Include Area Code)	22c. OFFICE SYMBOL
Major Joseph Hagger	202-767-4933	AFOSR/NE

DD FORM 1473, 83 APR EDITION OF 1 JAN 73 IS OBSOLETE.

TABLE OF CONTENTS

AIR FORCE OFFICE OF SCIENTIFIC RESEARCH (AFSC)
NOTICE OF

Chief, Technical Information Division

Dist

A-1

I. SUMMARY OF PROGRESS

During the second year of contract, a range of compositions from the C-Ti alloy system have been melted, and their physical and mechanical properties measured for comparison with theoretical predictions. These C-Ti alloys were produced using induction melting techniques. The alloys contained between 0 and 25 atom percent (0 to 7 weight percent) carbon. Optical metallography examination, hardness tests, compression tests and scanning electron microscopy have been performed on these alloys. The alloys were found to be composed of three phases: alpha, gamma and a carbon-rich phase. Two of the three phases are consistent with the postulated phase diagram. The third carbon-rich phase is thought to be a nonequilibrium component resulting from inhomogeneities during the melting process.

Compression tests conducted on specimens cut from the melts have room temperature ultimate tensile strengths between 50 and 165 ksi and strains to fracture between 1.5 and 10%. The strength of the C-Ti alloys increases and the ductility decreases with increasing C content. This is consistent with theoretical predictions. Experiments have also shown that the size and morphology of the gamma phase controls the strength and ductility in the composition range investigated. Alloys of the same 5 w/o C composition have been produced with ductilities of 5 to 10% and UTS of 165-100 ksi respectively by control of the gamma phase morphology. The 5-7 w/o carbon alloys have measured melting temperatures between 2000 and 2300 degrees centigrade. These are the highest melting temperature alloys now obtainable with present equipment.

II. OBJECTIVE OF RESEARCH

The objective of this research is to investigate a new class of material composed of 30-60 atomic percent carbon (C-Ti) for ultrahigh temperature applications in space power systems. The alloy system under investigation exhibits melting temperatures in excess of 2500 degrees C and form long range ordered structures which are expected to yield materials with exceptional high temperature strength and resistance to environmental degradation.

III. INTRODUCTION

The generation of power in space by methods other than direct conversion (photovoltaic) will require new concepts in materials to obtain optimum performance. Traditional materials used in the construction of land based power systems such as zircaloy, stainless steel, and in some exotic applications, Nb and V steels, do not have the necessary combined ultrahigh temperature strength, irradiation resistance, and strength to weight ratios that are required. The space reactor will operate in a near perfect vacuum, eliminating oxidation problems which plague many high temperature materials (Mo, V, etc.). However, sublimation of the materials (vaporization at high temperatures) will become a controlling factor. In space, the rejection of heat must occur by radiation of energy to the environment, requiring temperatures of 1000 degrees C or greater for thermodynamic efficiency. Additionally, the materials are required to withstand the radiation of the nuclear core (be resistant to irradiation induced densification, swelling and creep) and be lightweight for transportation into space.

Viewing the above general requirements, carbon based materials (C materials) are a superb candidate for development. C fiber - C matrix materials have been highly successful on the space shuttle where they have been used for components ranging from cargo bay doors to high temperature

motor casings. Such materials, however, are not suited for applications which require exposure to nuclear radiation. Testing in the high temperature gas cooled reactor program has identified two problems with C materials.

The first is the permeability of the C material to radioactive fission gases [1,2]. Despite the development of ultrahigh density C materials, special C coatings, and differential pressurization of components, leakage of C clad fuel occurs after very short neutron exposures ($\phi t < 1 \times 10^{22}$ n/cm^2).

Heat pipe components, fabricated from pure C or C composite materials, would therefore be unable to maintain proper partial pressures for operation. The second problem results from volumetric changes (densification) that occur in C materials upon neutron irradiation [1]. These changes are highly orientation dependent. The C fibers, which contain material with the basal planes aligned perpendicular to the stress axes, undergo a substantially different volumetric change than the matrix material, leading to the generation of high internal stress, cracking and ultimate failure. A class of materials which promise to overcome the above described problems is ordered C-metal alloys. Ordered alloys offer many potential advantages over conventional alloys at elevated temperatures [2-5]. The atomic ordering produces a pronounced increase in the work hardening [5-9], improves the fatigue resistance [10], and retards, because of stronger binding and closer packing of atoms, most thermally activated processes such as creep and grain growth [11]. In addition, the strength of ordered alloys is less sensitive to temperature than conventional disordered alloys. In fact, some alloys show an increase rather than a decrease in strength with increasing temperature up to the critical ordering point [12]. The critical ordering point is the temperature at which the material reverts from a defined periodic arrangement of alloying elements to the random arrangement found in conventional materials. Electron, ion bombardment, and recent neutron irradiation results

show the long range ordered (LRO) alloys to be highly swelling resistant [13-15].

Despite the above advantage, the LRO alloys have seen only limited application because of a lack of ductility associated with the ordered state [16-18]. Recently Liu and his coworkers at ORNL have succeeded in producing (Fe, Ni)$_3$V long range ordered alloys which show tensile elongations greater than 30% [19-21]. This has been achieved by controlling the ordered lattice structure through use of the e/a ratio or average electron density per atom outside the inert gas shell.

Ordered C-metal alloys represent a new approach which combines the desirable qualities of C (high temperature resistance, low weight, low vapor pressure) with the radiation and permeability resistance of ordered materials. These alloys, containing 30-60 atomic percent carbon, all exhibit melting temperatures in excess of 2500 degrees C [22,23]. By careful control of the alloy composition, desirable ordered structures can be maintained at temperatures in excess of 0.7 Tm (approx. 1800 degrees C). The alloys will be relatively lightweight, yet resistant to irradiation damage. Control of the ordered structure by modification of the e/a ratio will produce compositions with good ductility, strength, creep and fatigue properties. In addition, the C-metals will eliminate the permeability problem associated with pure C materials.

The objective of this research is to investigate the property-structure relationships of ordered C-metal alloys. These studies will provide a theoretical and experimental basis from which a future development program, leading to optimization and detailed characterization of ordered C-metal alloys, can be initiated.

IV. PROGRESS DURING THE SECOND YEAR OF THE PROJECT

The principle accomplishments during the second year of the project deal with experimental achievements. Based upon the proposed project plan, the research is on schedule. The work herein described was performed by two graduate students seeking Master's of Science degrees in Materials Engineering. These students are K. C. Yeh and Pamela Gills. Pamela joined the research project in June of 1983 and K. C. Yeh in September of 1984.

Approximately seventy-five percent of the second year effort was spent fabricating and investigating the mechanical properties of the 0 to 7 weight percent C alloys of the C-Ti system. These alloys had been identified theoretically and through scoping experiments to have the greatest potential during the first year of the contract. Fifteen percent of the second year effort was used to characterize the material microstructure, deformation mechanisms and fracture surfaces. The remaining ten percent was used to continue development of theoretical models for comparison and prediction. The following sections will describe the progress made during the last year in the experimental investigation.

Experimental progress:

The C-Ti system was identified as the most promising alloy system based upon its ability to obtained an ordered structure over a range of compositions and its ultrahigh melting temperature (3080 degrees C). During this second year of the project, C-Ti alloys containing between 0 and 7 weight percent carbon were fabricated to investigate the physical and mechanical properties of the C-Ti system. Six compositions were melted (melting points ranging from 1650 degrees C to near 2300 degrees C) covering the range 0 to 7 weight percent carbon. The alloys melted did not include additions for improvement

of ductility. Experiments showed that significant ductility could be obtained by controlling the microstructure through heat treatment. For the 5 w/o C alloys, the ductility was varied between 4 and 10 percent by altering the size of the gamma phase. Hence it was deemed premature to begin investigations into the addition of alloying elements. The pure C-Ti alloys enable a direct comparison between theoretical prediction of ordering parameters and experiment. Unlike the experiments conducted during the first year of the contract, melts during the second year were made by induction melting techniques under an inert cover gas.

<i> The Production of C-Ti Alloys

Titanium and graphite sp-1 powder was placed into a graphite crucible approximately .51 inches in diameter and 1.34 inches high. The crucible and powder was placed into a quartz tube (inside diameter = .63 inches, outside diameter = .71 inches) that contains a tantalum sheet encircling the inside diameter. The crucible was placed within the tantalum sheet and supported in this location by a ceramic rod. The tantalum sheet serves principally as a radiation reflector but additionally serves as a gettering material to protect the melt from oxidation. The graphite crucible is the susceptor and quartz tube serves as the containment of the inert gas atmosphere. The bottom ceramic rod was used to limit heat transfer by conduction out of the crucible.

The quartz tube with crucible is placed within the 0.8 inch diameter copper coil of the induction generator. The diameter of the copper coil with respect to the diameter of the graphite crucible is critical in that these parameters determine the coupling that can be obtained between the induction generator and crucible and hence maximum temperatures. Higher temperatures are obtained as the diameter of the coil and crucible are decreased. This creates a problem in itself in that the size of the melt is decreased and the

fabrication and testing of specimens becomes more difficult. Additionally, the fabrication of the induction coils is greatly increased. The process of making small diameter coils involves continued twisting of coils from large diameter to small diameter gradually.

An infrared sensor is used to monitor the temperature of the melt. This sensor is suspended from the top support of the heating system. Fig. 1 and Fig. 2 show the system in operation. An argon atmosphere was maintained in the quartz tube during heating and cooling of the specimen. A graphite bar was used to stir the fluid alloy mixture to increase the diffusion of carbon into titanium, enhancing the formation of a homogeneous material composition and reducing porosity of the melts. The alloys in the 0 to 7 w/o C region were produced using an induction generator set to provide a direct current of 40 amps at 230 volts. Samples were limited in size to less than 6 cubic cm by the experimental requirement to reach high temperatures. The maximum temperature that can be obtained using this system is 2300 degrees C. This procedure can melt compositions containing up to 7 w/o carbon. However, it is difficult to reach temperatures higher than 2100 degrees C routinely. The inability to reach higher temperatures will be corrected after purchase of a larger capacity induction generator is completed.

<ii> Optical Metallography

Figures 3 through 6 show representative microstructures of the C-Ti alloys produced by the above described induction melting procedure. Figure 3 is the photomicrograph of a 4 weight percent (w/o) carbon-titanium alloy. Figures 4 through 6 are microstructures of alloys with increasing carbon content (5 w/o to 7 w/o). The figures show that the microstructures consist principally of a mixture of alpha-Ti and gamma phases at room temperature. A third carbon rich phase was found in some of the higher carbon percentage
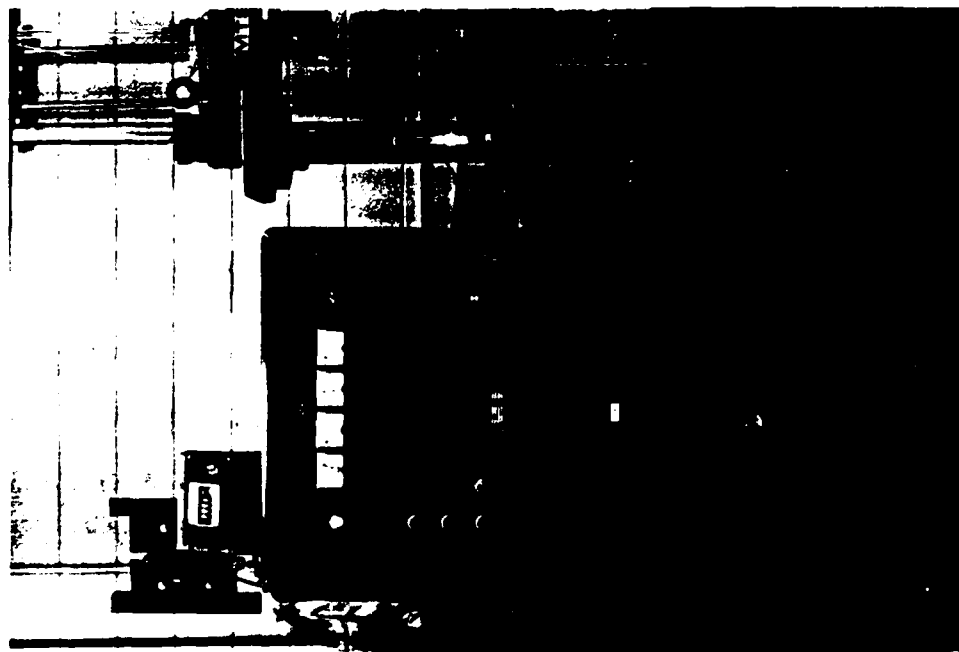
Figure 2: Closeup of induction melting coil, crucible and quartz tube.

Figure 1: Induction generator and melting furnance used to produce Ti-C alloys.

Figure 3: Transverse photomicrograph of
Ti-4 w/o C alloy. Globular
phase is gamma-phase. Volume
fraction of alpha-Ti is 69%.

A
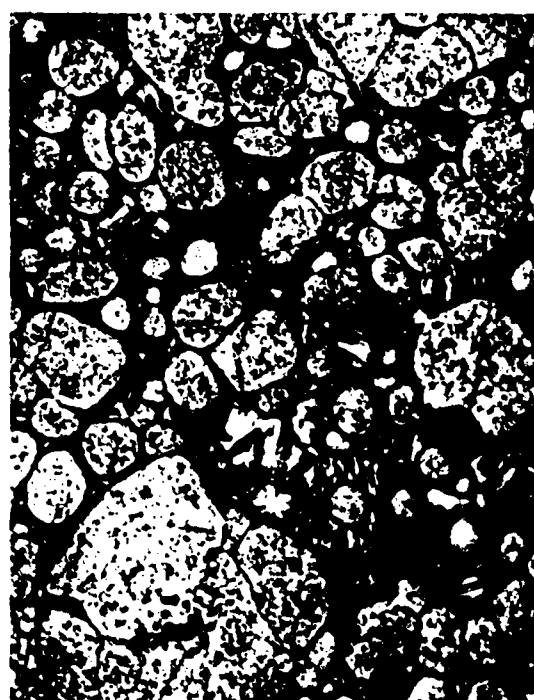
B

Figure 4:   Transverse photomicrograph of Ti-5 w/o C alloy.
A received rapid cool from melt resulting in a
uniform size and distribution of gamma phase.
B received slow cool from melt producing some
very large gamma phase particles. Volume frac-
tion of of alpha-Ti is 54 and 50% respectively
for A and B.

Figure 6: Transverse photomicrograph of Ti-7 w/o C alloy. Volume fraction of alpha-Ti is 49%.

Figure 5: Transverse photomicrograph of Ti-6 w/o C alloy. Volume fraction of alpha-Ti is 52%.

alloys and is thought to be the result of localized incomplete diffusion of carbon into the melt. Figure 7 is the phase diagram for the C-Ti system. By comparing the results with the published phase diagrams for the C-Ti system, the findings show agreement with the anticipated phases and the microstructure for the alloys of 4 to 7 w/o carbon with the above noted exception of the high carbon content phase. Figures 8 through 12 show the gamma-phase particle size distribution and the volume fraction of alpha-Ti (4-7 w/o C). From these figures, we found that the total number of gamma-phase particles decreases and particle size increases as the carbon content is increased. When the carbon content is increased, larger particles of gamma phase tend to form. In addition, the volume fraction of gamma phase increases as the carbon content is increased. Because of this, the strength of C-Ti alloys increases.

<iii> Hardness Measurements

Hardness measurements were made on the alloys as one of the tests to characterize their mechanical properties. The macroscopic hardness measurements were found to vary with carbon content and as a function of processing treatment. The rockwell C hardness varied from a value of 25 for a 4 w/o carbon alloy to 35 for the 7 w/o carbon alloy. In addition to macrohardness measurements, microhardness measurements were made on the alpha-Ti and gamma phase structures seen in the photomicrographs of figures 3 through 6. The diamond indentations on the alpha-Ti phase were very clear and large, but they appear small on the gamma phase and are difficult to measure. Figure 13 and figure 14 compare the microhardness of alpha-Ti and gamma phases from the Ti-4 w/o C and Ti-7 w/o C alloys. From this data it is concluded that the microhardness of gamma phase increases as the carbon content is increased. The Knoop hardness values of alpha-Ti are insensitive to carbon

C-Ti   Carbon-Titanium
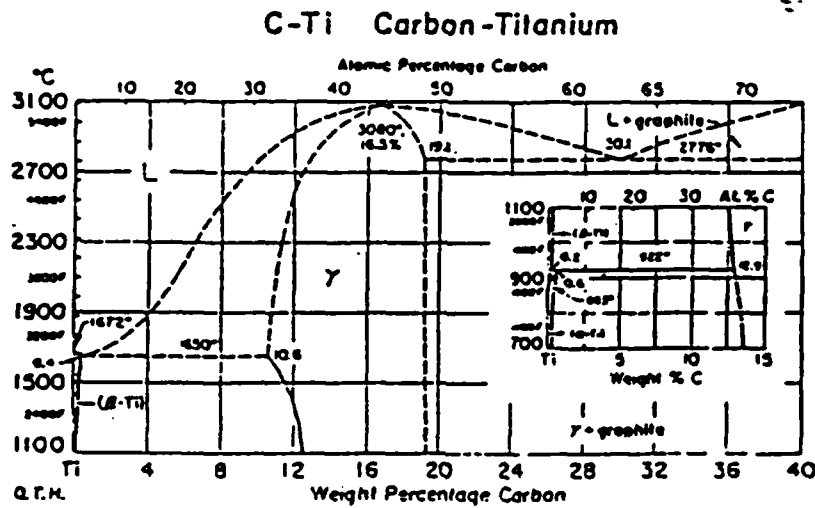
from reference 22

Figure 7: Phase diagram for the C-Ti alloy
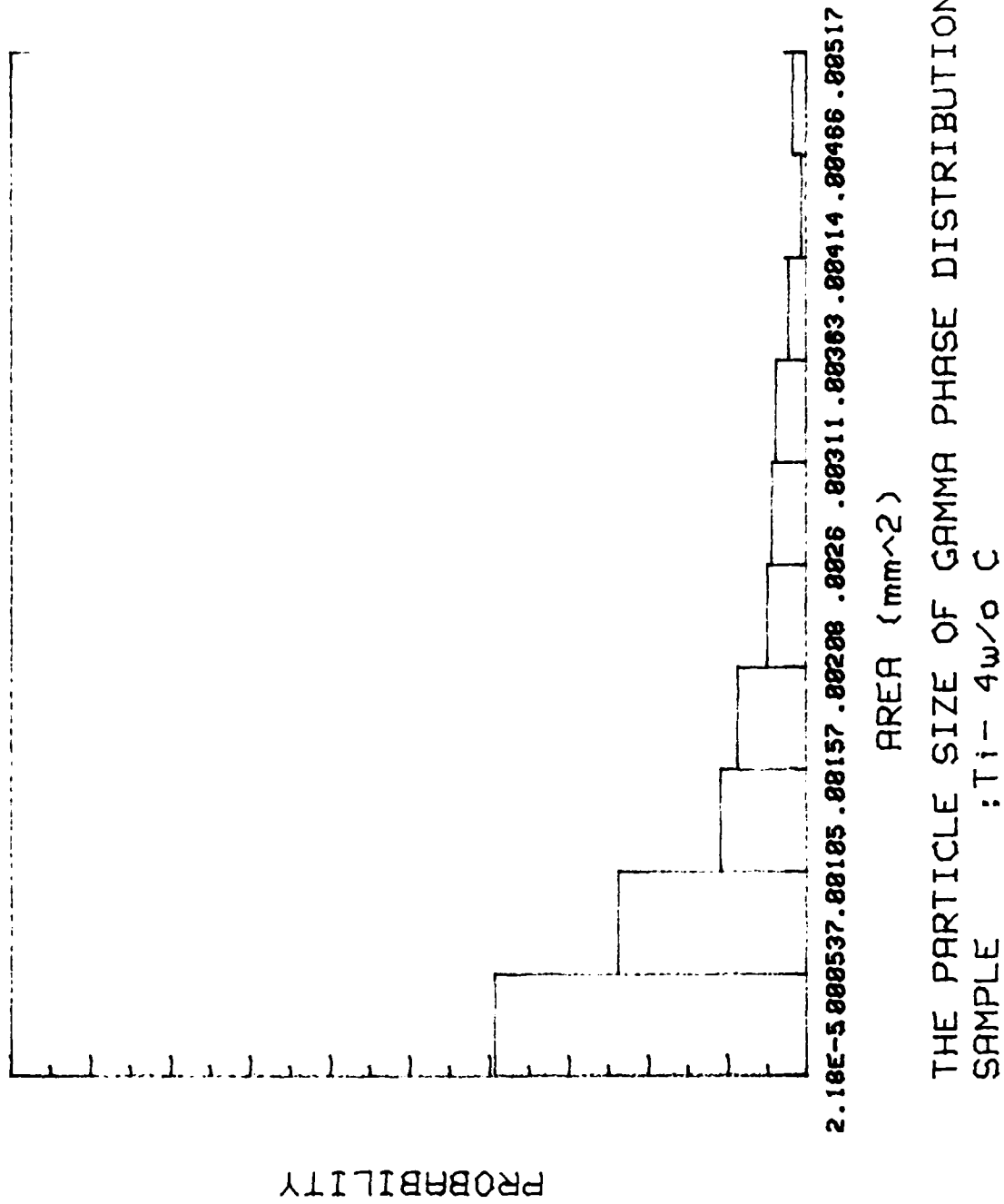system. Note that the dashed lines
indicate calculated phase relations.

THE PARTICLE SIZE OF GAMMA PHASE DISTRIBUTION

SAMPLE :Ti- 5w/o C

AREA (mm^2)

PROBABILITY

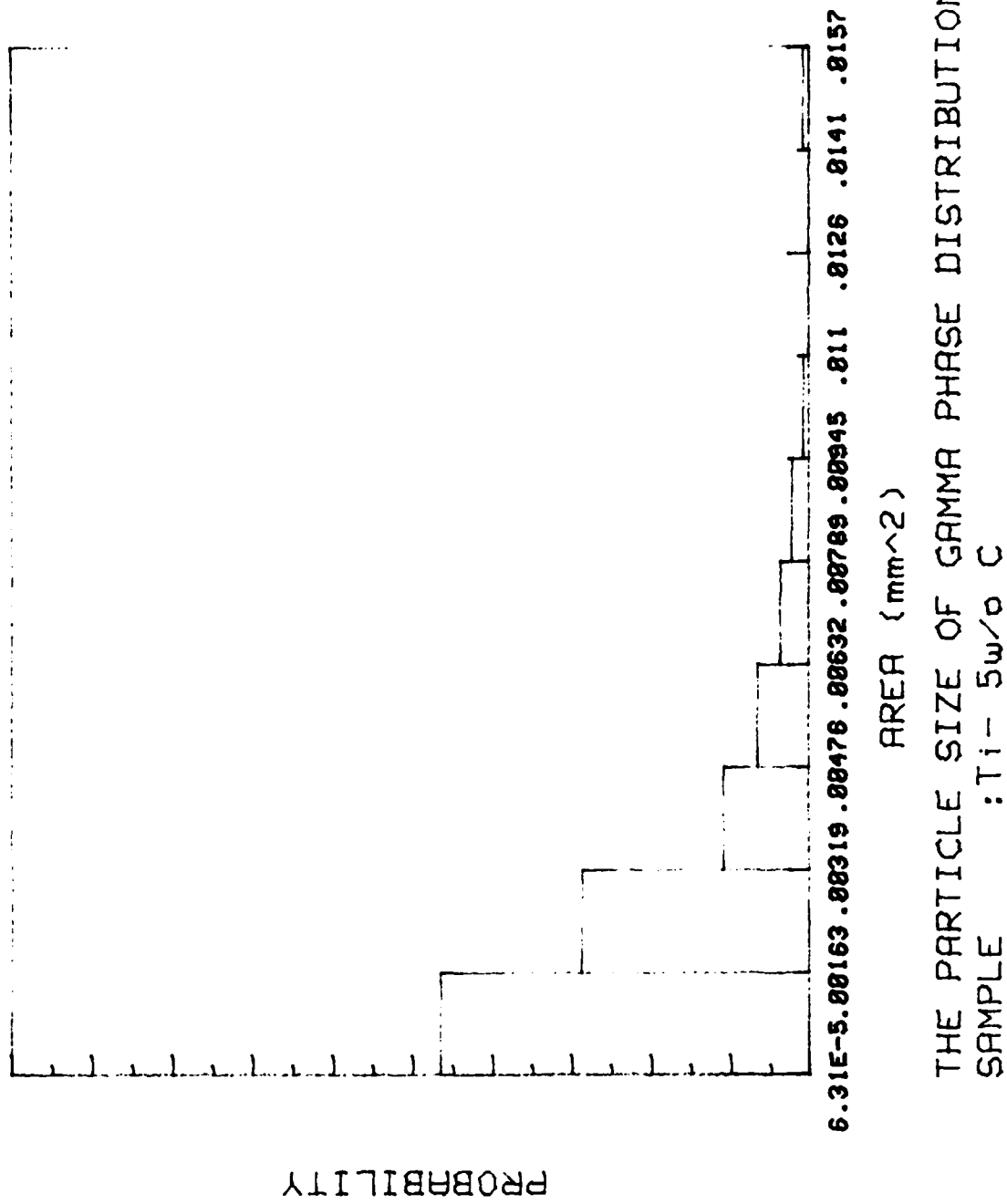6.31E-5 .00163 .00319 .00476 .00632 .00789 .00945 .811 .8126 .8141 .8157

Figure 9: Gamma Phase Size Distribution: Rapid Cooled Ti-5 w/o C. Microstructure of alloy shown in Fig. 4A.

GAMMA PHASE FRACTION: 45.88 %
ALPHA PHASE FRACTION: 54.12 %
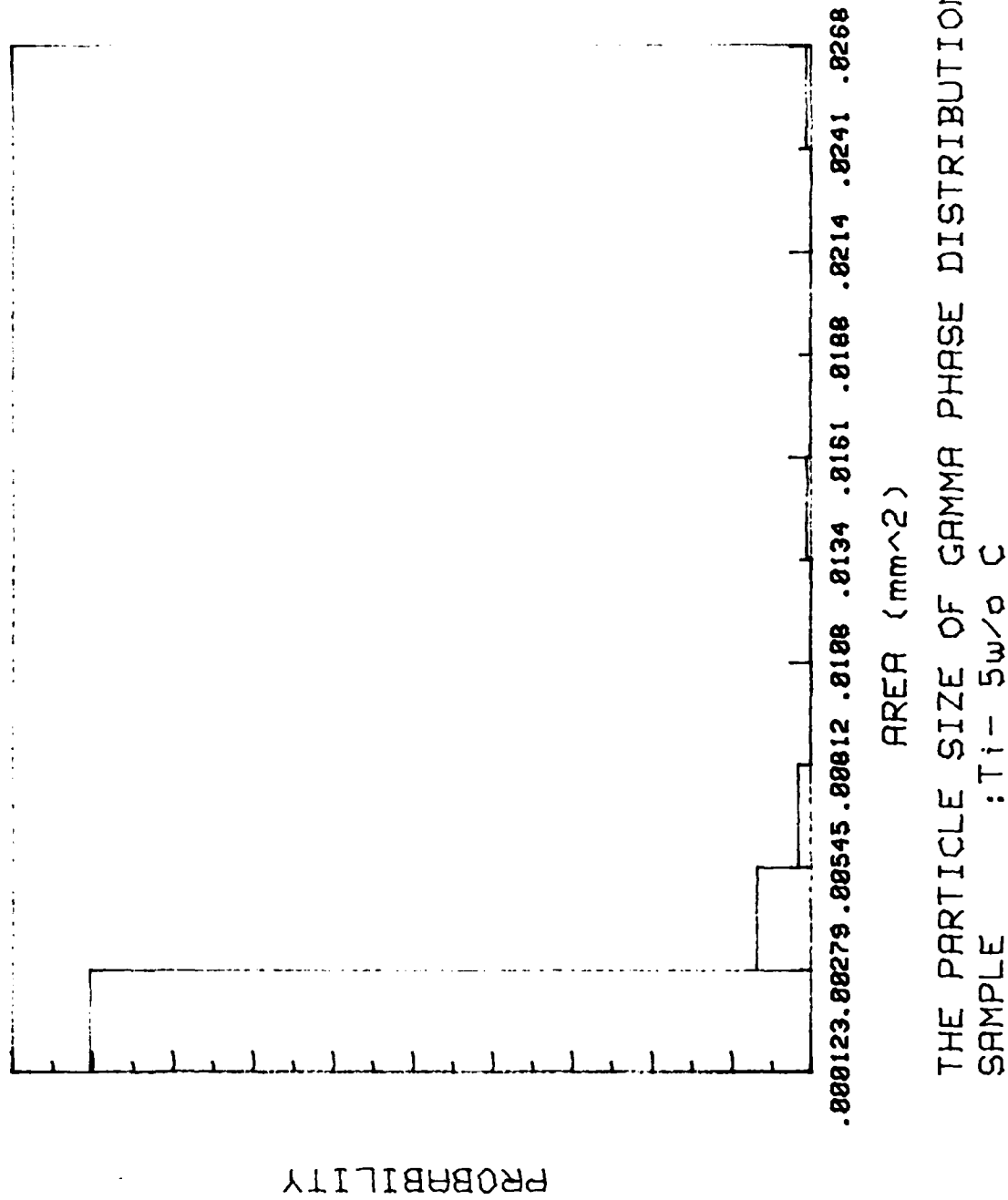TOTAL PARTICLE NO. : 140
AVERAGE OF AREA: .0023672031 (mm^2)

THE PARTICLE SIZE OF GAMMA PHASE DISTRIBUTION
SAMPLE   :Ti- 5w/o C

AREA (mm^2)

.000123.00279.00545.00812.0188 .0134 .0161 .0188 .0214 .8241 .0268

PROBABILITY

Figure 10: Gamma Phase Size Distribution:Slow
Cooled Ti-5 w/o C. Microstructure
of alloy shown in Fig. 4B. Note
almost bimodel distribution of
gamma phase particle size.

GAMMA PHASE FRACTION: 50.39 %
ALPHA-Ti FRACTION : 49.61 %
TOTAL PARTICLE NO. : 194
AVERAGE OF AREA: .0013908847 (mm^2)

THE PARTICLE SIZE OF GAMMA PHASE DISTRIBUTION

SAMPLE :Ti-6w/o C

AREA (mm^2)

.00013 .00157 .00301 .00445 .0059 .00734 .00878 .01022 .0117 .0131 .0145
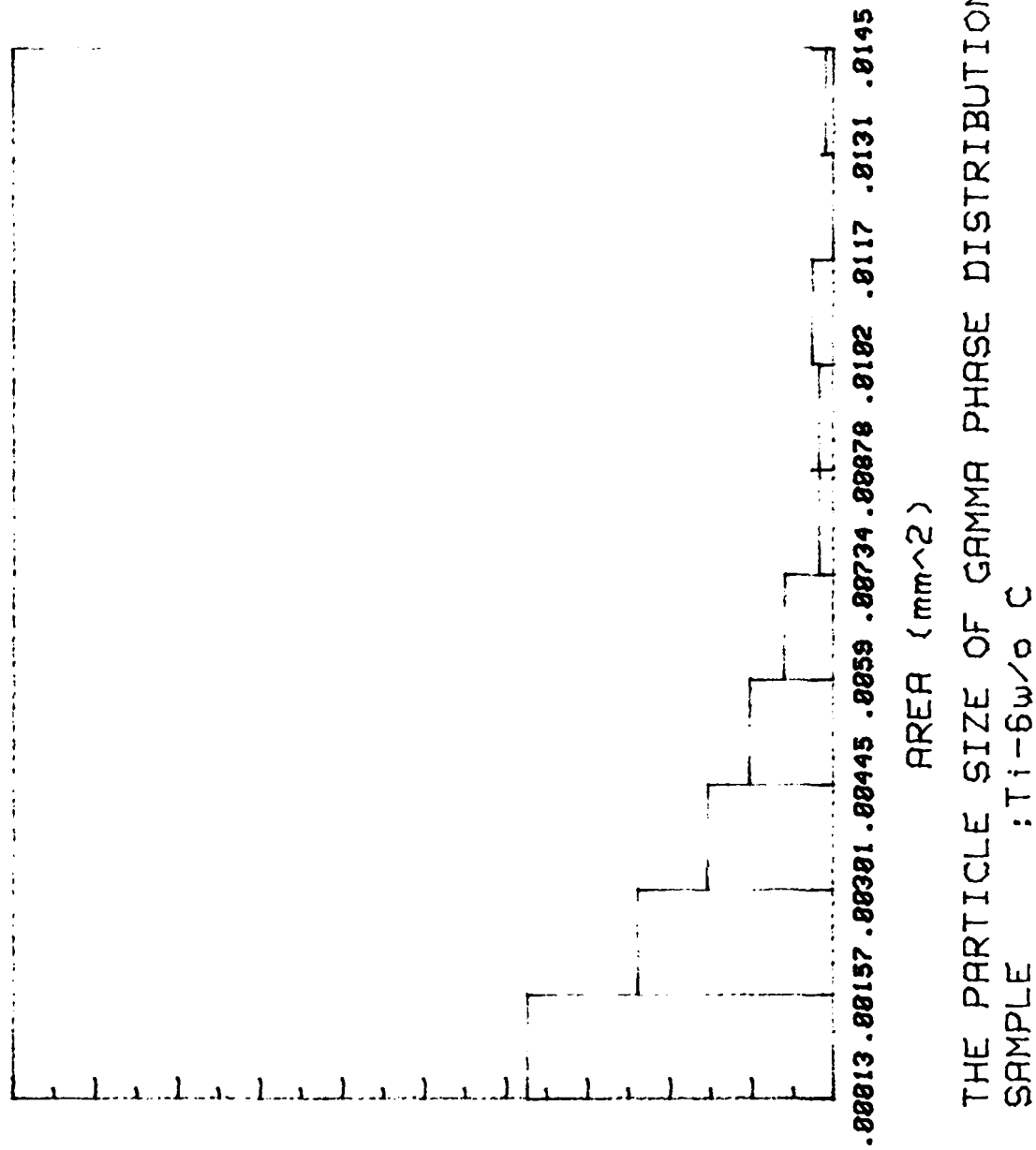
PROBABILITY

Figure 11: Gamma Phase Size Distribution : Ti-6 w/o C. Microstructure shown in Figure 5.

GAMMA PHASE FRACTION: 49.94 %
ALPHA PHASE FRACTION: 50.06 %
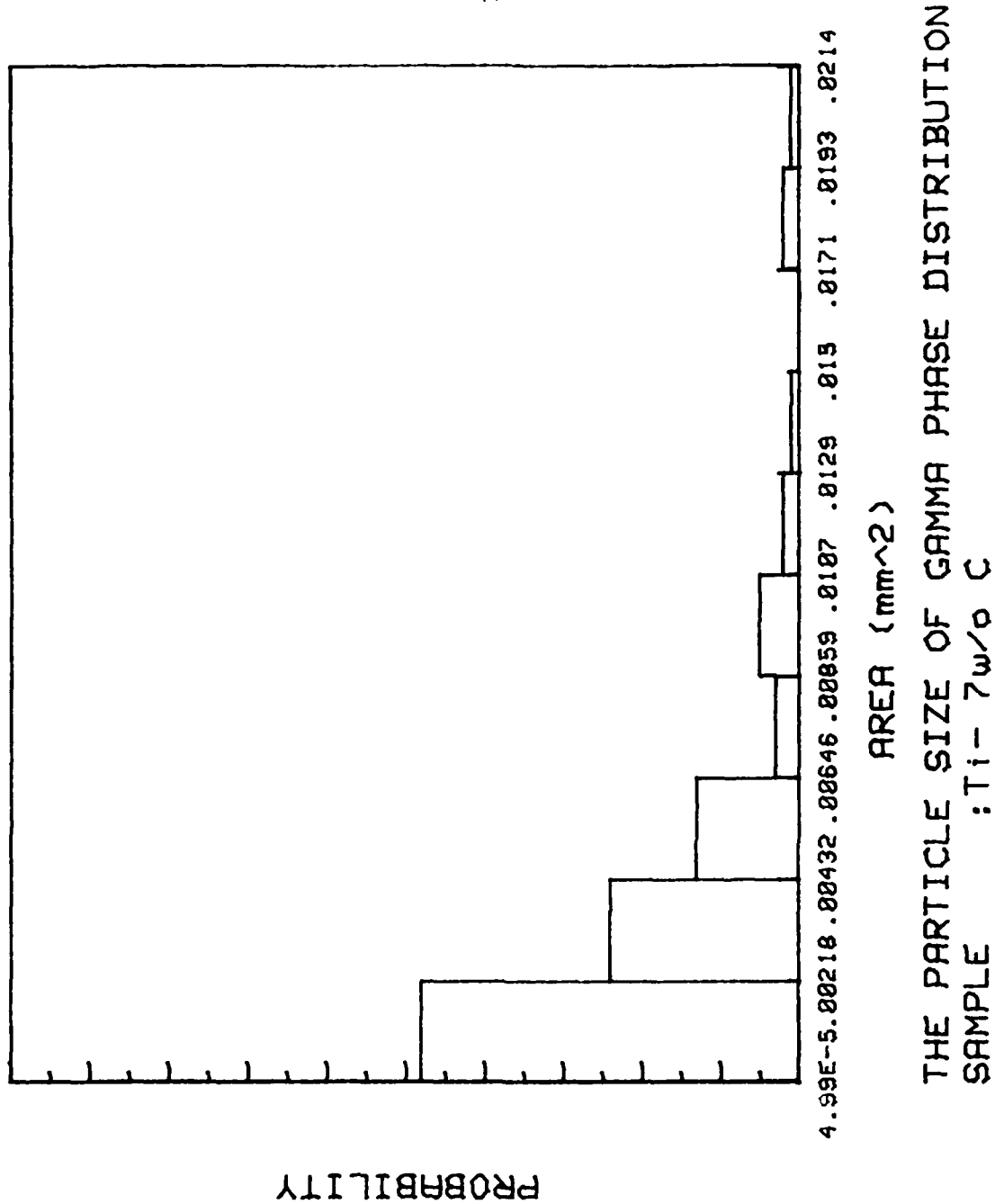TOTAL PARTICLE NO. : 118
AVERAGE OF AREA: .0030005189 (mm^2)

Figure 12: Gamma Phase Size Distribution
: Ti-7 w/o C. Microstructure
shown in Figure 6.
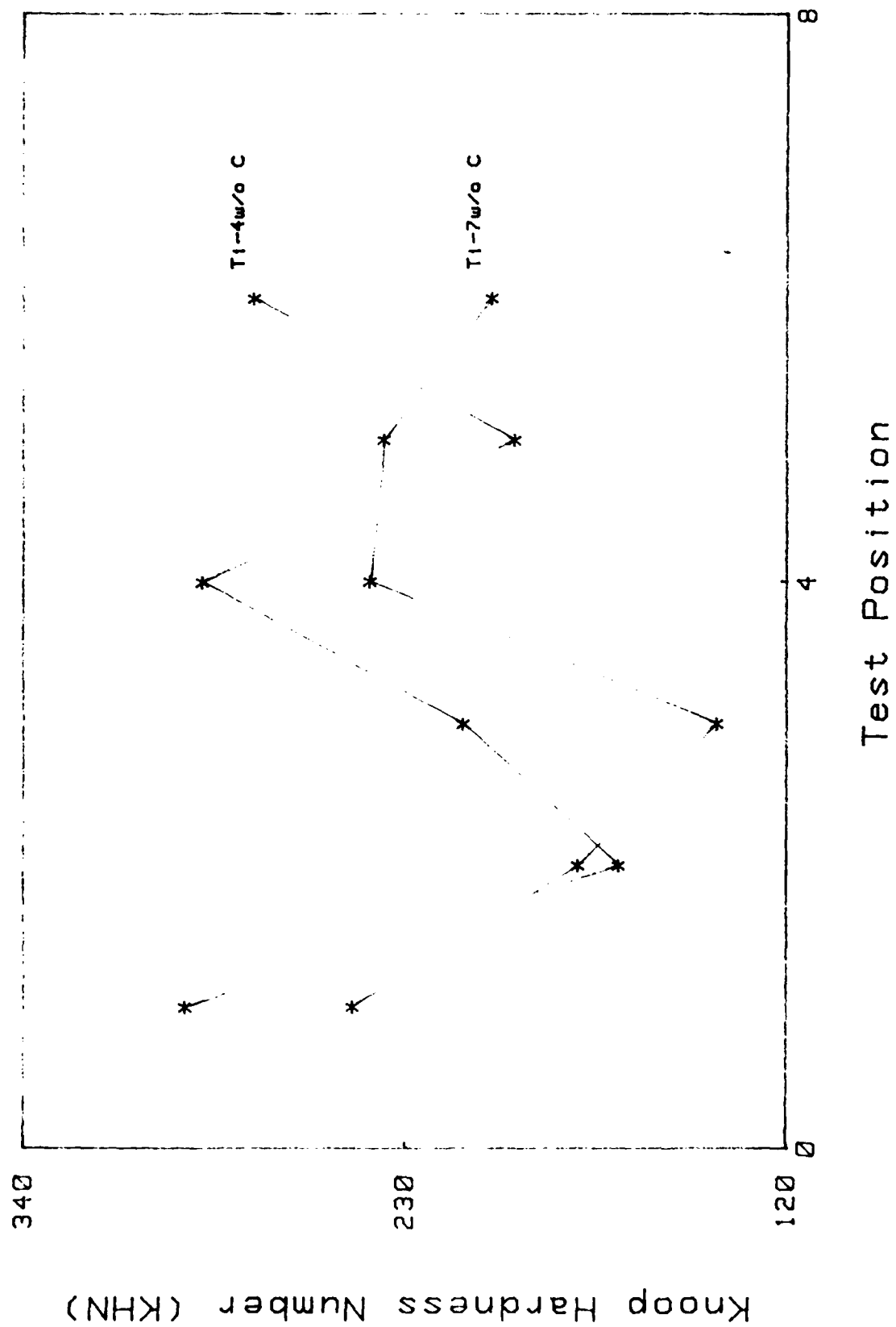
Figure 13: Microhardness tests of alpha-Ti.
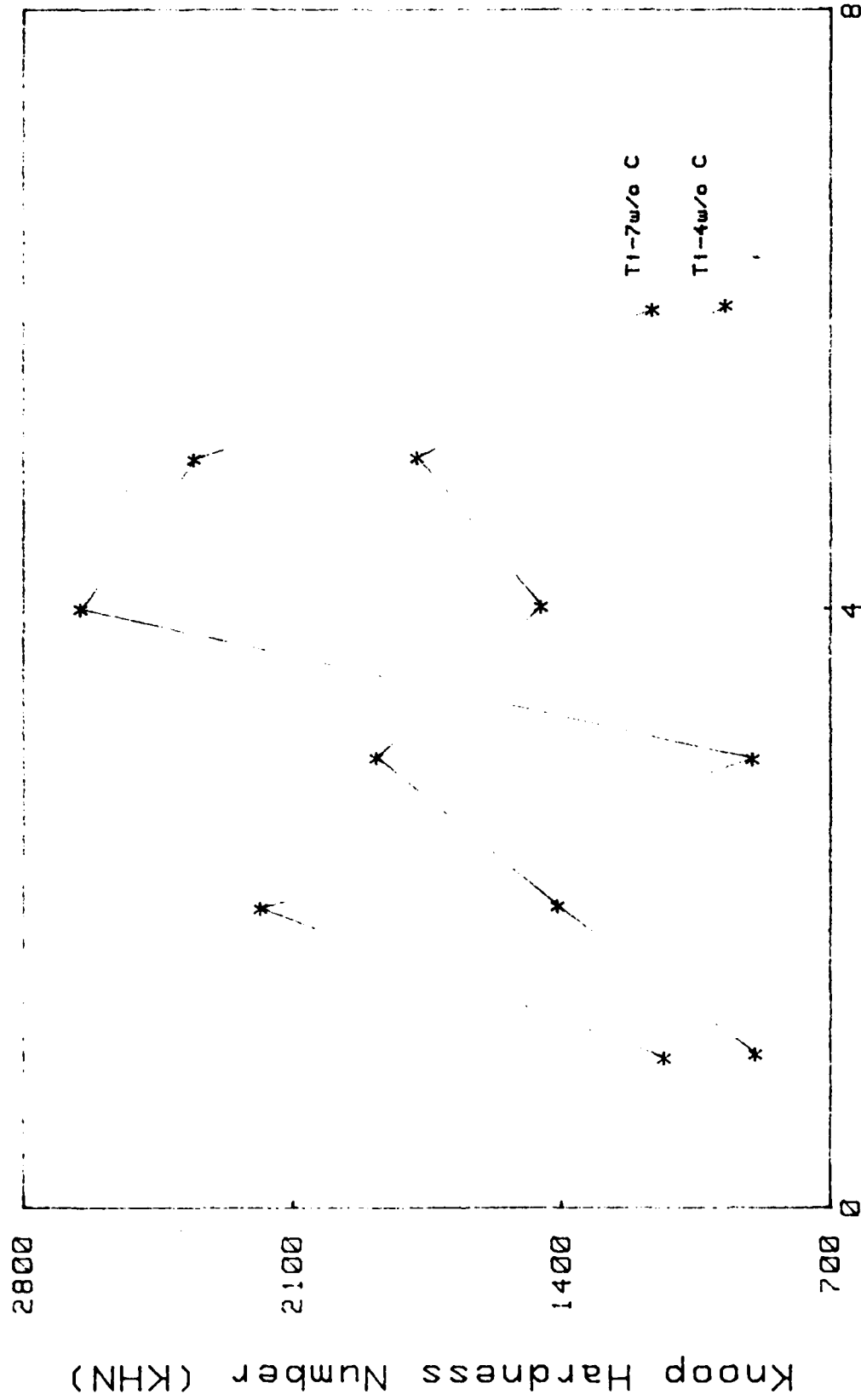
Figure 14: Microhardness tests of gamma phase.

content. The strength of C-Ti alloys is therefore dictated by the volume fraction and distribution of gamma phase.

<iv> Compression Tests

Techniques have been developed for the fabrication of ASTM subsize compression specimens from C-Ti alloys. Because of the small size and properties of the available material, a diamond impregnated soft core tube which has an inside diameter of 6.4 mm was used to prepare cylindrical compression specimens. The drill utilizes water as a lubricant and coolant to protect the samples from overheating. After a cylinder is cut from the melt, a diamond slitting saw was used to cut both ends of the cylinder to length and obtain parallel ends. The alloys were gummy in nature, thus requiring sharpening of the diamond blade with a carbon block to remove cut particles stuck in the blade. Although the alloys were not excessively hard, large amounts of time were required to prepare the cylindrical compression sample, which measured 4.45 mm diamater by 12.7 mm high. A diameter to length ratio of 2.71 to 2.96 were used for all tested specimens. These specifications meet ASTM STANDARDS for subsize compression samples [24]. Prior to compression testing, specimens were ultrasonically cleaned in acetone. Compression tests were conducted at room temperature under stroke control using a Material Testing System (Figure 15). The data were simutaneously recorded on a HP X-Y chart recorder and through a digital HP 9836 data acquisition system. The larger size gamma phase particles control the strength and ductility.

A summary of the mechanical properties of tested titanium-carbon alloys is given in Table 1. Figure 16 and figure 17 show a typical compression specimen before and after testing. Macroscopic failure occured along a 45 degree plane similar to that of previously reported rectangular shaped Ti-4w/o C specimens. From Table 1 and Figure 18 it can be seen that there are two
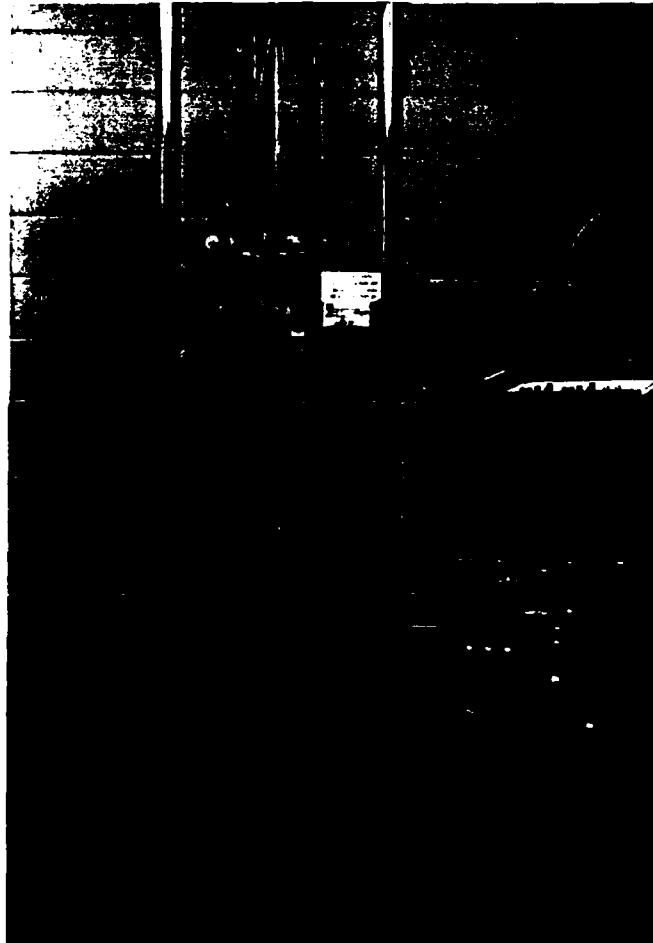
Figure 15: Compression tests were conducted
using a Materials Testing System
with data acquisition by a HP 9836
computer system.

Table I

Summary of Average Mechanical Properties
for 0-7 w/o C-Ti Alloys

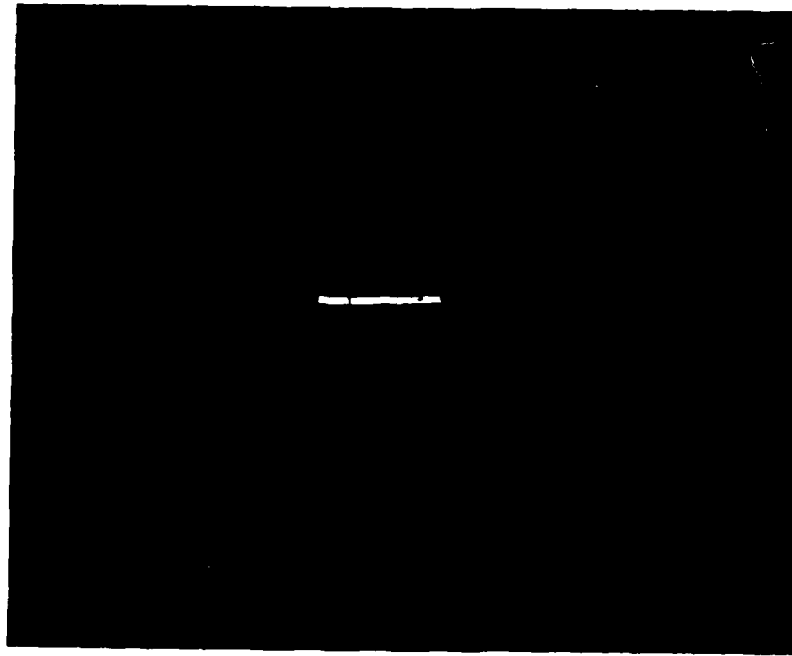| Alloy	Cond	Melting Temp.(^{0}C)	Yield	UTS	Strain to Fracture	Hardness
Ti	cast	1665	20	34	54.0	70 HB
Ti-4C	slow cool	1900	42	54	1.4	41R_c
Ti-5C	slow cool	2000	100	165	5.0	32R_c
Ti-5C	rapid cool	2000	75	100	10.0	28R_c
Ti-7C	rapid cool	2250	90	100	5.0	35R_c
Ti-6A1-4V	cast	1650	120	130	4.0	32R_c

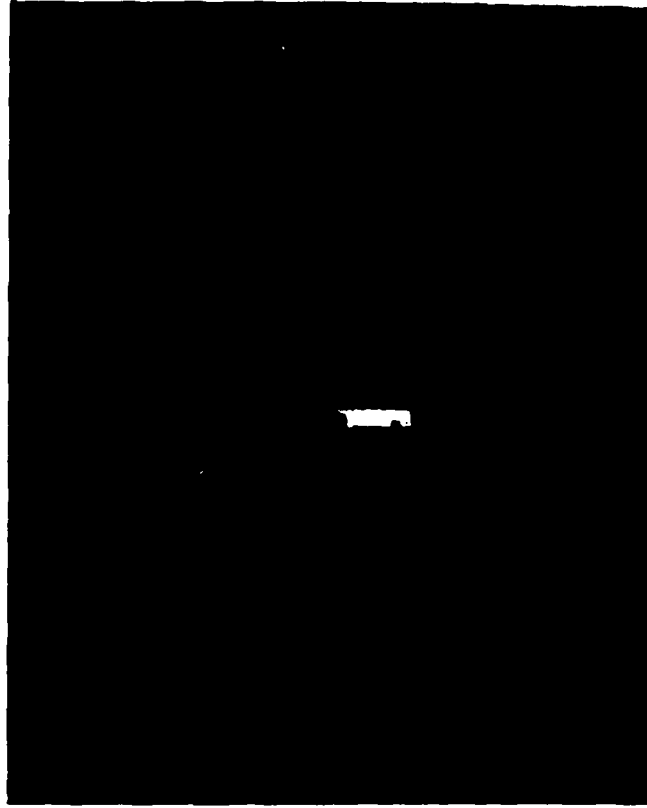Figure 17: Compression test sample after test.
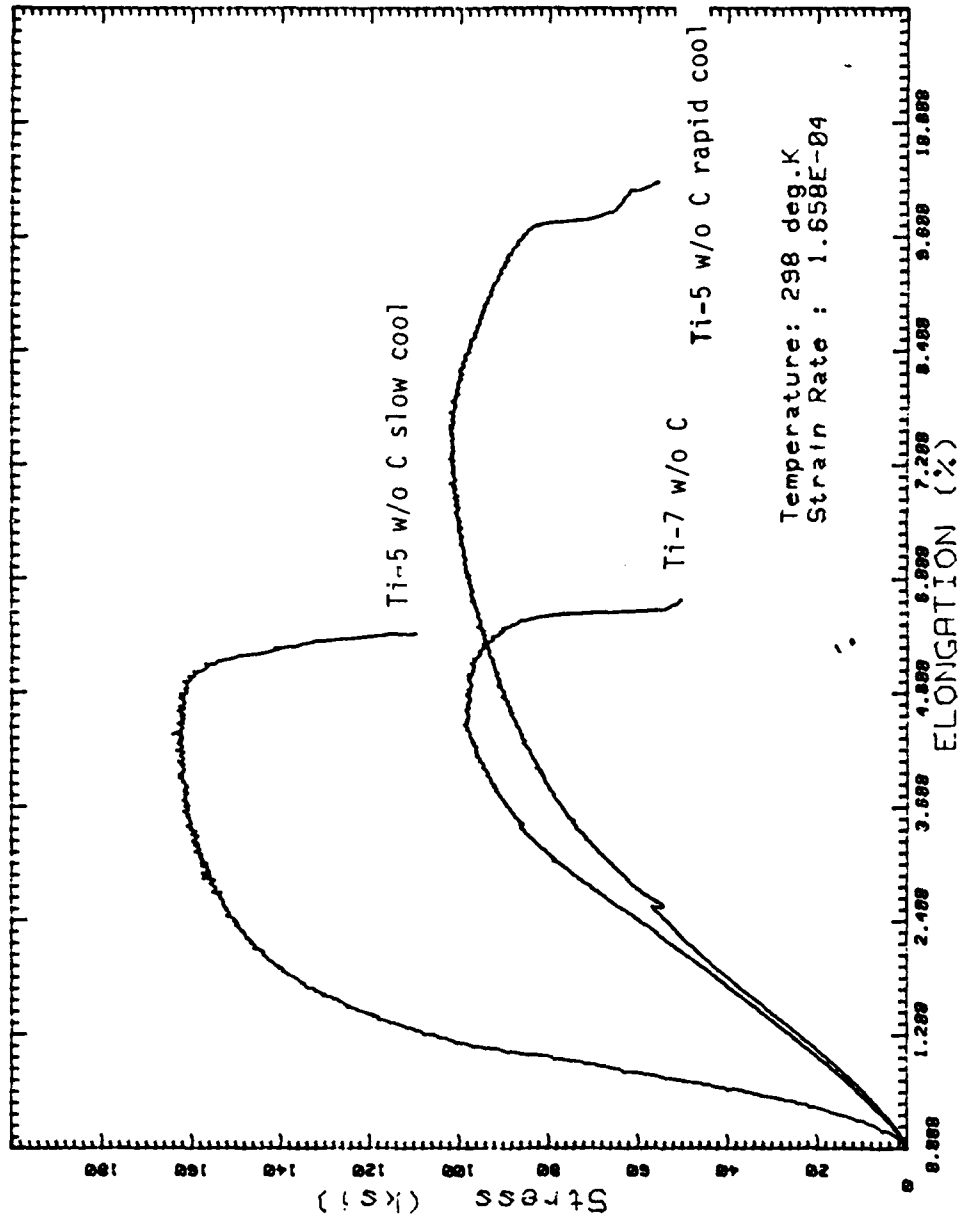

Figure 16: Compression test sample before test.

Figure 18: Stress Strain Compression Curves for 5 w/o C alloys (rapid and slow cool) and 7 w/o C alloy.

series of compression tests with immensely different mechanical properties for the same alloy. This data demonstrate that fabrication processes can be used to control the properties of the Ti-C materials. One series of specimens have a UTS of 165 ksi and 4.5% strain to failure while the second set shows a UTS of 105 ksi and nearly 10% strain to failure. A strain to fracture of 10% is very surprising and suggests that achieving ductile Ti-C alloys may not require other element additions. This ductility is the result of a different microstructure seen in Figures 4A and 4B in the section on metallography.

Minimum melting temperatures have been established by referenced infrared thermography. The reference point used to calibrate the emmissivity was the melting point of pure Titanium material, 1668 degrees C. Values of the minimum melting point temperatures for the 0-7 w/o C alloys are also shown in Table 1. Figure 18 is the stress strain curve for the compression test of the 5 w/o and 7 w/o carbon specimens. The properties of the alloys show that the elongation of C-Ti alloys, as expected, decreases as the carbon content is increased.

<v> Fracture Surface Observation

Figures 19 through 26 show the fracture surfaces of typical 5 and 7 w/o carbon alloys tested in compression. Examination of the fractographs indicate that there are significant amounts of cleavage failure in the 5 w/o carbon alloy. Additionally, cleavage fracture is much greater in the 7 w/o carbon alloy than the 5 w/o alloy. Striations along the surface shown in figure 19 (5 w/o carbon) and figure 24 (7 w/o carbon) were produced during the final failure of the specimen. The micrographs of both alloys show regions of craters, the bottom of the craters show smooth surfaces indicative of failure by cleavage. These features suggest that failure has occurred along the boundary between alpha Ti and gamma phases. The appearence of large cracks
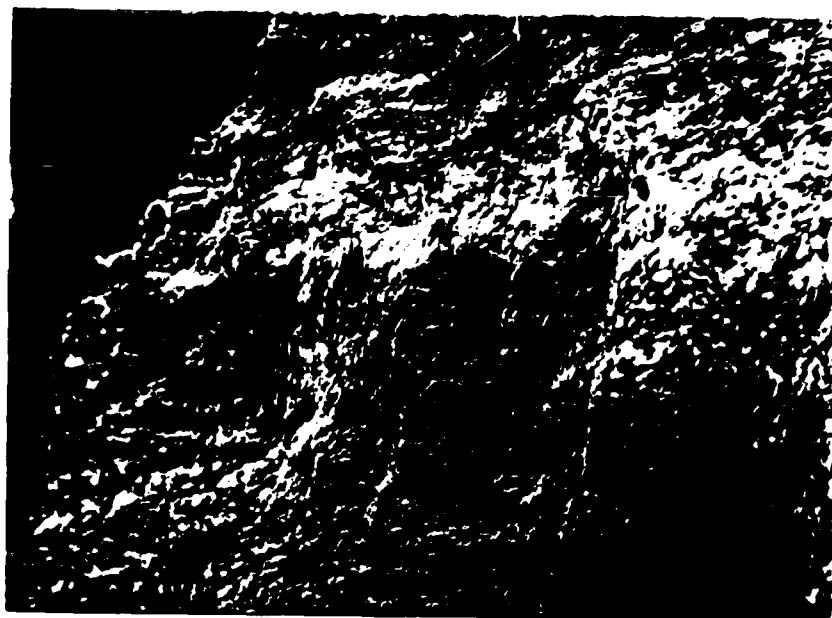
Figure 19: Complete cross section of fracture
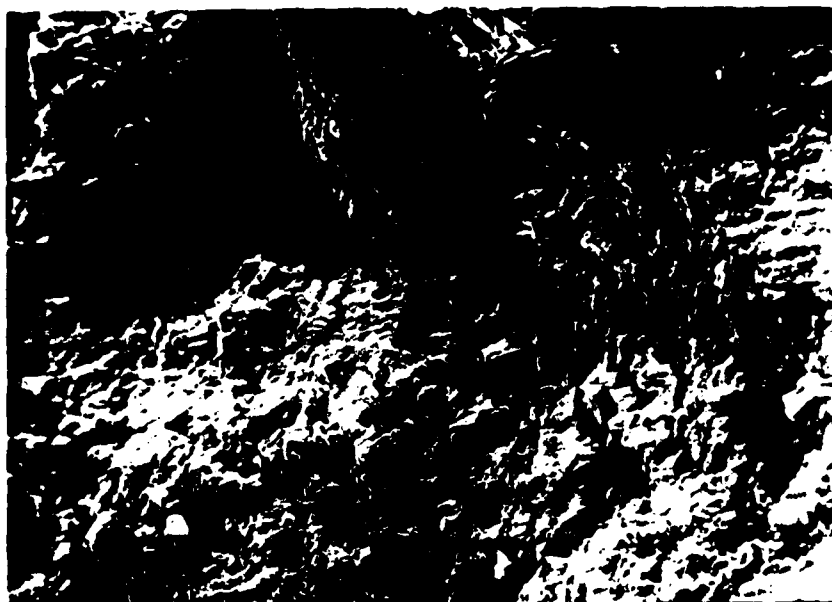surface of 5 w/o C alloy.

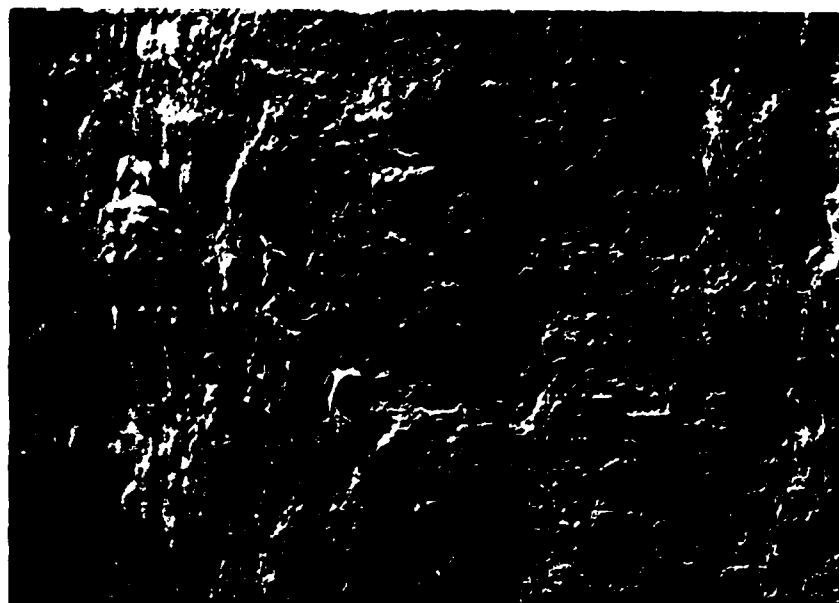Figure 20: Top right hand region of figure 19
(higher magnification).

Figure 21: Central region of figure 19
(higher magnification).

Figure 22: Bottom left hand region of figure 19
(higher magnification).

Figure 23: Complete cross section of frac-
tion surface of 7 w/o C alloy.

Figure 24: Top right hand region of figure 23
(higher magnification).

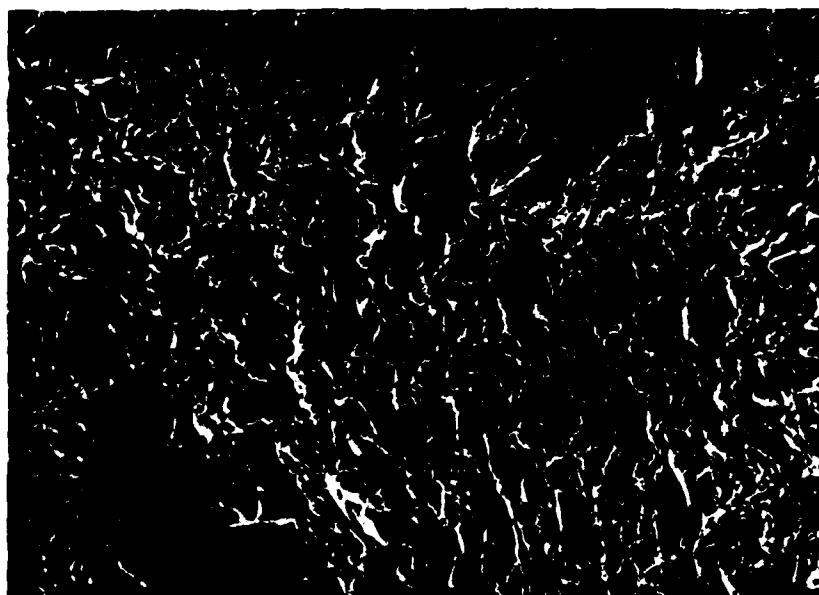Figure 25: Central region of figure 23
(higher magnification).

Figure 26: Bottom left hand region of
figure 23 (higher magnification).

extending into the specimen regions of figure 20 and 24 show that final

failure occurred by the linking up of cracks on several planes. In the 5 w/o

alloy final failure occurred by linking up of cracks which initiated on

several planes. There is an abundance of secondary cracks which indicates

significant energy was expended in the initiation and propagation of these

cracks prior to final failure. In contrast the photomicrographs of the 7 w/o

carbon sample, figures 23 through 26 show failure occurred after linkage of

only a few large cracks on a few planes. Very little secondary cracking is

identified in this sample.

The fracture surfaces of all higher carbon content alloys show regions

which are different in fracture appearence. Some of this inhomegeneity is

attributed to lack of compositional uniformity in the melt. A more uniform

distribution of constituents is needed to improve the ductility and also

enhance the strength. Higher temperatures are needed to obtain a homogeneous

melt in the high carbon alloys.

V.   CONCLUSIONS

● C-Ti alloys covering compositions between 0 and 7 w/o carbon have been
   melted, fabricated and tested. Optical metallography shows that these
   alloys are composed of three phases: alpha titanium, gamma, and a carbon
   rich phase.

● Compression test results show that the ultimate tensile strength and
   strain to fracture can be varied between 105-165 ksi and 10-5%
   respectively by controlling the the size and distribution of the gamma
   phase in the 0-7 w/o carbon alloys.

● The fracture surfaces show a mixed mode of failure. Regions of cleavage
   appear to be the result of failure at the gamma-alpha phase boundary.

VI. REFERENCES:

1. F. J. Homan, "Fueled Graphite Development", Gas Cooled Reactor Programs, Annual Progress Report, ORNL-5753. August 1981, pg. 19.

2. N. S. Stoloff and R. G. David, "The Mechanical Properties of Ordered Alloys", Progress in Materials Science, Vol. 13, (1), 1966, pg. 1.

3. B. H. Kear, C. F. Sims, N. S. Stoloff, and J. H. Westbrook, Eds., Ordered Alloys Structure and Physical Metallurgy, Proc. 3rd Bolton Landing Conf., Lake George, N.Y., Claiter's Pub. Div. (1970).

4. M. A. Krivoglaz and A. A. Smirinov, The Theory of Order-Disorder in Alloys, American Elsevier Pub. Co., New York (1964).

5. F. Muto and Y. Takagi, The Theory of Order-Disorder Transformations in Alloys, Academic Press, New York (1956).

6. L. E. Popov and N. A. Koneva, Order Disorder Transformations in Alloys, J. Warlimont, Ed., Springer-Verlag, New York, (1974). pg. 404.

7. M. J. Marcinkowski, Order Disorder Transformations in Alloys, J. Warlimont, Ed., Springer-Verlag, New York, (1974), pg. 364.

8. A. E. Vidoz, D. P. Lazarenio and R. W. Chan, Acta Met, Vol. 11, (1963), pg. 17.

9. B. H. Kear and H. Wilsdorf, Trans AIME, Vol. 224, (1962), pg. 382.

10. R. C. Boetlnew, N. S. Stoloff, and R. G. Davis, Trans AIME, Vol. 236, (1966), pg. 131.

11. E. M. Schulson, "Order Strengthening as a Method for Reducing Irradiation Creep: An Hypothesis", Journal of Nuclear Materials, Vol. 66, (1977), pg. 322.

12. C. T. Liu, "Development of Iron-Base Alloys with Long Range Ordered Crystal Structure", ADIP Quarterly Progress Report, DOE/ER-0045/1, April, (1980), pg. 72.

13. D. N. Braski, "Resistance of (Fe, Ni) V Long Range Ordered Alloys to Radiation Damage", Alloy Development for Irradiation Performance, Proceedings of DOE Program Review Meeting, Sept. 30 - Oct. 1, (1980), pg. 367.

14. R. W.Carpenter and E. A. Kenik, "Stability of Chemical Order in N M Alloys Under Fast Electron Irradiation", in Proceedings of 35th Electron Microscopy Society, Claitor's Publishing, Baton Rouge, LA, 1977.

15. G. J. E. Carpenter and E. M. Schulson, J. Nuclear Materials, Vol. 23, (1978), pg. 180.

16. E. M. Schulson, J. Nuclear Material, Col. 56, (1975), pg. 38.

17. E. M. Schulson and M. H. Stewart, Met. Trans B., Vol. 78, (1976), pg. 363.

18. L. E. Tanner, P. Stark, E. T. Petters, J. J. Ryan, I. Vilks, and S. V. Radcliffe. AST-TDR62-1087, Man Labs Inc., Cambridge, MA 1963.

19. C. T. Liu, "Development of Long Range Ordered Alloys", Alloy Development for Irradiation Performance, Proceedings of Program Review Meeting, Sept. 30 - Oct. 1, 1980, pg. 354.

20. C. T. Liu and H. Inouye, "Control of Ordered Structure and Ductility of (Fe, Co, Ni) V Alloys", Met. Trans A., Vol. 10, (1979), pg. 1515.

21. C. T. Liu, "Development of Long Range Order", ADIP Quarterly Progress Report, DOE-ET-0058/1, August. 1978.

22. M. Hansen, <u>Constitution of Binary Alloys</u>, McGraw-Hill, New York, (1958), pg. 370.

23. T. Lyman, Ed., "Metallography, Structures and Phase Diagrams", <u>Metals Handbook</u>, Vol. 8 (1973), pg. 279.

24. American Society for Testing Material, "1958 Books of ASTM STANDARDS", Part 3 Methods of Testing Metals.

END

FILMED

1-86

DTIC